Analysis of pion scattering to stretched states in ^{60}Ni and other nuclei using Woods-Saxon wave functions

B. L. Clausen,* J. T. Brack, M. R. Braunstein, J. J. Kraushaar, R. A. Loveman,† R. J. Peterson, and R. A. Ristinen
Nuclear Physics Laboratory, Department of Physics, University of Colorado, Boulder, Colorado 80309

R. A. Lindgren
Institute of Nuclear and Particle Physics and Department of Physics, University of Virginia, Charlottesville, Virginia 22901

M. A. Plum
Los Alamos National Laboratory, Los Alamos, New Mexico 87545
(Received 24 July 1989)

Inelastic scattering of 162 MeV π^- and π^+ was used to study the previously known $J^\pi=8^-$ stretched transitions in ^{60}Ni. A consistent analysis of data from electron and pion scattering to stretched states using both harmonic oscillator and Woods-Saxon wave functions (unbound as necessary) was performed for ^{60}Ni and three other nuclei: ^{14}C, ^{28}Si, and ^{54}Fe. The experimental pion scattering cross sections were reproduced by distorted-wave impulse approximation calculations using wave functions from (e,e') with a normalization factor N that generally varied from 1 to 5. The ratio of the total isoscalar to the total isovector strength ranged from 0.2 to 1.2. The use of Woods-Saxon wave functions in the analysis did not significantly improve the fits to the angular distributions.

I. INTRODUCTION

It is well known that nuclear models based on the nuclear mean field theory have failed to explain the experimental strength of magnetic excitations in nuclei,[1-3] including high-spin "stretched" excitations. In these excitations the one-body spin transition density is basically composed of a single particle-hole configuration such as $(d_{5/2}p_{3/2}^{-1})4^-$ in ^{14}C, $(f_{7/2}d_{5/2}^{-1})6^-$ in ^{28}Si, and $(g_{9/2}f_{7/2}^{-1})8^-$ in ^{60}Ni. Although the strength is incorrectly predicted, the shell model in the framework of the distorted-wave impulse approximation (DWIA) does predict the correct q dependence of the electron scattering cross sections. By varying the strength of the stretched configuration until the calculated form factor fits the electron data, we can extract the strength of the transition in terms of a single isovector spectroscopic amplitude. This amplitude, which is deduced from (e,e') in a unique and unambiguous way, serves as a benchmark not only for comparison with results from more refined model calculations, but also for comparison with amplitudes deduced from other experiments using spin-sensitive probes for exciting the same transition.

In this study we are particularly interested in using inelastic pion scattering at energies near the $\Delta_{3,3}$ resonance to provide a test of the DWIA model for pion scattering and a test of our knowledge of the strength of the pion-nucleon spin-orbit interaction in the nucleus which allows us to predict pion-nucleus scattering cross sections. Previous pion studies using harmonic oscillator (HO) radial wave functions for stretched excitations in self-conjugate nuclei, required a normalization of the total calculated cross section by factors that ranged from 1.1 (^{28}Si) to 1.4 (^{14}C),[4,5] in order to obtain the same strength as in electron scattering. The fact that these normalization factors vary from unity suggests that there are still inadequacies in the model of pion scattering from the nucleus and/or in the nuclear structure of the proton and neutron wave functions. Although the radial transition density is taken from electron scattering which is sensitive to the entire radial distribution, there still may be difficulties because the HO wave functions do not take into account effects due to differences between the proton and neutron wave functions. This is particularly important for unbound states, because differences in the radial wave functions are large at the nuclear surface where the pion scattering amplitudes are strong. Such effects can be accounted for using a Woods-Saxon (WS) potential,[6-10] including continuum effects as noted in the past,[11] but not thoroughly tested. To improve our understanding of the pion-nucleus scattering model, we present systematic analyses of previous ^{14}C, ^{28}Si, and ^{54}Fe data and include new ^{60}Ni data. Several specific objectives are discussed next.

The first is to conduct a systematic analysis of electron[12] and pion excitations of the pure isovector and isoscalar stretched transition in the ^{28}Si (Refs. 8 and 13) self-conjugate nucleus using both HO and WS wave functions in the DWIA model of pion scattering, and including effects due to the unbound nature of the states. The sensitivity of the extracted Z_1 and Z_0 coefficients and the overall normalization to these radial wave functions will

be studied.

The second objective is to deduce the isovector (Z_1) and isoscalar (Z_0) contributions for magnetic transitions to T_0 states in the ^{14}C (Refs. 4 and 14–16) and ^{54}Fe (Refs. 17 and 18) non-self-conjugate nuclei by using the ratio of π^+ and π^- cross sections to give Z_0/Z_1 and the electron cross sections to give essentially Z_1. (This includes the one T_0+1 state in ^{54}Fe.) The advantage of this technique is that the two sets of solutions for Z_0 and Z_1 are essentially independent of the absolute strength of the pion-nucleon interactions, but dependent on the *well known* ratio of the isoscalar to isovector part of the pion-nucleon interaction near resonance. This is particularly complementary to electron scattering, since the pion cross section is 4 times more sensitive to isoscalar states than isovector states having the same internal structure.

The third objective is to present and analyze the small, inelastic pion scattering cross sections for exciting the stretched 8^- transitions in ^{60}Ni by pion scattering (see Ref. 19 for more details). These data together with ^{60}Ni electron data[20] are used to extract Z_0 and Z_1 and, consequently, can be used to make isospin assignments for the 8^- states in ^{60}Ni. Work on this nucleus is of special interest because this is the first published report for pion scattering on a nucleus with $T_z=2$ in contrast to $T_z=0/1$ for nuclei used in earlier studies. As a result, the simple shell model sum rule for the isovector strength predicts that the T_0 strength is twice that of the T_0+1 strength, unlike $T=1$ nuclei, where it is evenly divided between $T=1$ and $T=2$ states.

II. THE ^{60}Ni (π,π') DATA

A. Experimental details

The experiment was performed by bombarding an enriched ^{60}Ni target of areal thickness 94.3±2 mg/cm^2 with a beam of 162 MeV pions from the energetic pion channel and spectrometer (EPICS) at the Clinton P. Anderson Meson Physics Facility (LAMPF), which has been described in previous work.[21] Inelastic pion scattering cross sections were measured at spectrometer angles of 65°, 80°, and 90° for π^+ and 65° and 80° for π^- with an energy resolution [full width at half maximum (FWHM)] of 190 keV and with the spectrometer field set so that pions causing an excitation energy of 12.8 MeV (the average energy of the known stretched states) would be detected at the center of the focal plane.

A three-quarter frame target of Ni and a one-quarter frame target of CH_2 were initially used for π^+ and π^- runs at a scattering angle of 80° to insure that the energy calibration of the Ni spectra was done correctly. Once the calibration seemed satisfactory, a full frame Ni target was used to expedite data acquisition and a full frame C target was inserted occasionally as a calibration check. During the data analysis, it was found that all carbon calibration runs at a given scattering angle were similar; therefore, they were added together to give one summed spectrum at each angle.

The individual nickel spectra are shown in Fig. 1 along with a summed spectrum used to facilitate finding the stretched states. The energy calibration of the summed spectrum utilized peaks corresponding to the ground state and the strong 2^+, and 3^- excited states in ^{60}Ni (1.333 and 4.040 MeV) and ^{12}C (4.439 and 9.641 MeV). The resulting energies of the 8^- states are shown in Table I. These energies are equal within uncertainties to those found previously in electron scattering[20] and proton stripping.[22] In the five individual nickel spectra, the stretched state peaks were fit using the excitation energy from the summed spectrum, the width and skew of the elastic peak, and a linear background. An acceptance correction and a pion survival fraction correction were done bin by bin on the histograms before any peak fitting was done.

The 8^- cross sections were normalized to previously known $\pi+p$ and $\pi+^{12}$C elastic scattering cross sections.[23,24] The normalization factor was 0.90 smaller for π^- cross sections at a given angle than for π^+ cross sections, which is similar to results of Seestrom-Morris at 160 MeV.[25] As a further check, we found that the ^{12}C inelastic scattering cross sections were in agreement with previous work.[26] Moreover, the ^{60}Ni cross sections for low lying states (see Table I) were similar to those in ^{58}Ni.[27] The total systematic error is about 10%, with 7% due to uncertainties in the absolute normalization. The errors listed in Table I include statistical as well as these

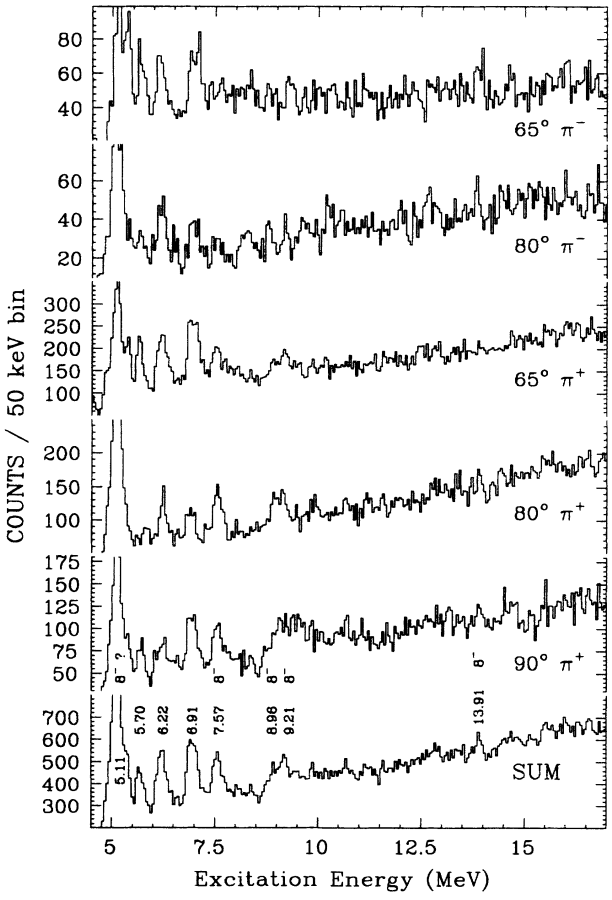

FIG. 1. The π^- and π^+ spectra from ^{60}Ni as well as the summed spectrum. The 8^- stretched transitions observed in electron scattering are labeled along with several other prominent states. Each channel is 50 keV wide.

TABLE I. Measured excitation energies and center-of-mass cross sections for the states observed in ^{60}Ni pion scattering. Energies with uncertainties are from this experiment. The scattering angles are given in the center-of-mass frame. The listed cross section uncertainties include both statistical and systematic errors. The 8^- assignments are those of Lindgren *et al.* (Ref. 20).

	J^π	E_x (MeV)	$\sigma^\pm$ (μb/sr) 65.3°	80.3°	90.3°
π^-	0^+	0.00	3100 ±300	76 ± 7	
	2^+	1.33	33 ± 4	140 ±20	
	3^-	4.04	250 ± 20	30 ± 3	
	8^-	5.11±0.02	61 ± 6	38 ± 4	
		5.70±0.04	30 ± 4	11 ± 2	
		6.22±0.02	23 ± 4	16 ± 2	
		6.91±0.02	26 ± 4	12 + 2	
	8^-	7.57±0.02	9.9± 3.6	6.7± 1.5	
	8^-	8.96±0.03	4.2± 3.3	3.3± 1.5	
	8^-	9.21±0.03	9.2± 3.6	5.0± 1.7	
	8^-	13.91±0.04	15 ± 4	5.7± 2.3	
π^+	0^+	0.00	1500 ±100	230 ±20	110 ±10
	2^+	1.33	91 ± 6	100 ±10	18 ± 2
	3^-	4.04	180 ± 20	19 ± 2	35 ± 3
	8^-	5.11±0.02	44 ± 3	34 ± 3	25 ± 2
		5.70±0.04	19 ± 2	4.1± 0.8	6.3± 0.9
		6.22±0.02	20 ± 2	8.9± 1.1	6.1± 0.9
		6.91±0.02	22 ± 2	5.9± 1.0	8.7± 1.1
	8^-	7.57±0.02	8.4± 1.6	9.5± 1.1	6.3± 1.1
	8^-	8.96±0.03	6.7± 1.5	6.6± 1.1	5.8± 1.0
	8^-	9.21±0.03	8.4± 1.5	4.6± 1.0	6.7± 1.1
	8^-	13.91±0.04	3.0± 1.6	4.5± 1.2	3.3± 1.1

systematic uncertainties.

The pion cross section measurements are given in Table I and angular distributions are shown in Fig. 2. Of the ten states identified as stretched states in electron scattering, only the 7.5, 9.0, and 9.2 MeV T_0 states and the 13.9 MeV T_0+1 state were observed in pion scattering. Our ability to distinguish the other six states from background is questionable.

B. The 5.1 MeV state

Four peaks between 5 and 7 MeV were also analyzed in the hope of finding new 8^- isoscalar stretched transitions not observed in electron scattering. Their cross sections are listed in Table I. Unfortunately, the angular distributions in this experiment are not complete enough to make definitive assignments of multipolarity. However, from the angular distributions listed in Table I, the 5.7 and 6.9 MeV states do not appear to be 8^- candidates. A recent EPICS experiment by Oakley *et al.*[28] using 180 MeV pions on ^{60}Ni was able to add to our angular distributions. A 6.22 MeV state was observed with a cross section of at least 40 μb/sr at 30° and 35° for both pion signs, thus removing it as a possible 8^- candidate. Another state was observed at 5.24 MeV with a cross section of 250±40 μb/sr at both angles and pion signs. This is probably the 5.24 MeV 4^+ state mentioned by Ronsin *et al.*[29] (They also mention a 5.106 MeV 4^+ state.) If the 5.24 MeV state found by Oakley *et al.* is assumed instead to be a doublet, any 5.1 MeV state appears to have

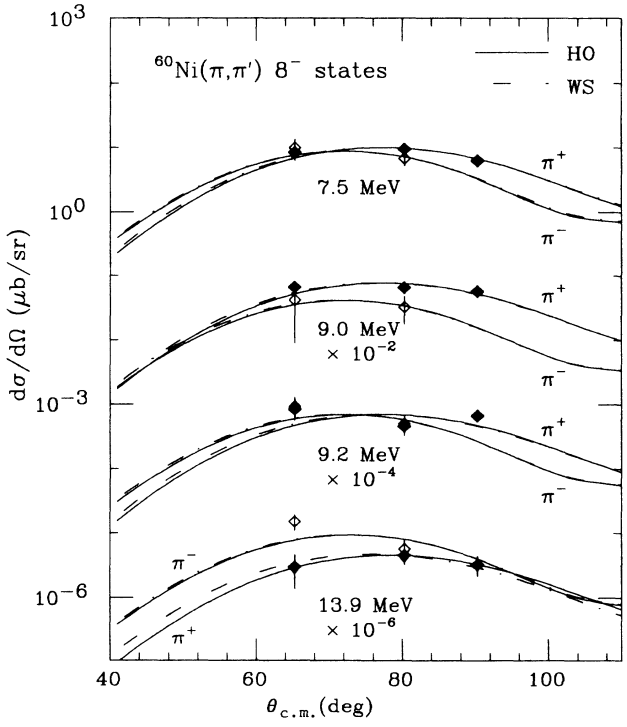

FIG. 2. Pion angular distributions calculated with HO and WS wave functions are compared to data for the 8^- stretched transitions in ^{60}Ni. Open diamonds are the π^- data; solid diamonds are the π^+ data.

a negligible cross section, but at most could have 200 μb/sr for π^+ at both angles, 120 μb/sr at 30° π^-, and 36 μb/sr for 35° π^-. Figure 3 compares the 5.1 MeV data from both experiments with HO theory curves for 8^- and 4^+ angular distributions. (For the small difference between 180 and 162 MeV pions, the shift in scattering angle is negligible for our purposes.) The HO parameter used was $b = 1.95$ as found to fit the other ^{60}Ni stretched transitions. The data are more consistent with an 8^- assignment, so the 5.1 MeV state is tentatively included as an 8^- stretched transition in this paper. Also note that for the 5.1 MeV state, $\sigma^- \approx \sigma^+$ as expected for a pure isoscalar transition.

III. ANALYSIS

A. Inelastic scattering differential cross sections

The inelastic pion-nucleus scattering cross sections for exciting unnatural parity states at pion energies near the $\Delta_{3,3}$ resonance are calculated in the distorted-wave impulse approximation (DWIA) using the formalism described by Petrovich, Carr, and McManus.[3] In this model the pion-nucleus coupling is given by the usual central and spin-orbit terms, but only the latter contributes to unnatural parity states. We have also neglected the higher order, presumably weaker spin-current and current coupling terms associated with nonlocalities arising from the energy dependence of the spin-orbit term and nuclear Fermi motion. Although these higher order terms are small in general, their weakness is also justified on the important assumption that the one-body transition density does not contain any significant $\Delta N = 3\hbar\omega$ or higher particle-hole configurations. From core polarization calculations[30] in ^{28}Si, calculated values of Z^2 for $\Delta N \geq 3$ are less than 1% near the peak of the form factor. In addition, there is no experimental evidence from the shape of electron scattering form factors for stretched transitions to indicate that higher order configurations are required to fit the data near the peak of the form factor. In fact, form factors calculated from the pure $1\hbar\omega$ configuration fit the data well past the maximum for all of the strong transitions; therefore, any effects requiring orbital coupling densities, including the known dependence, can be neglected.

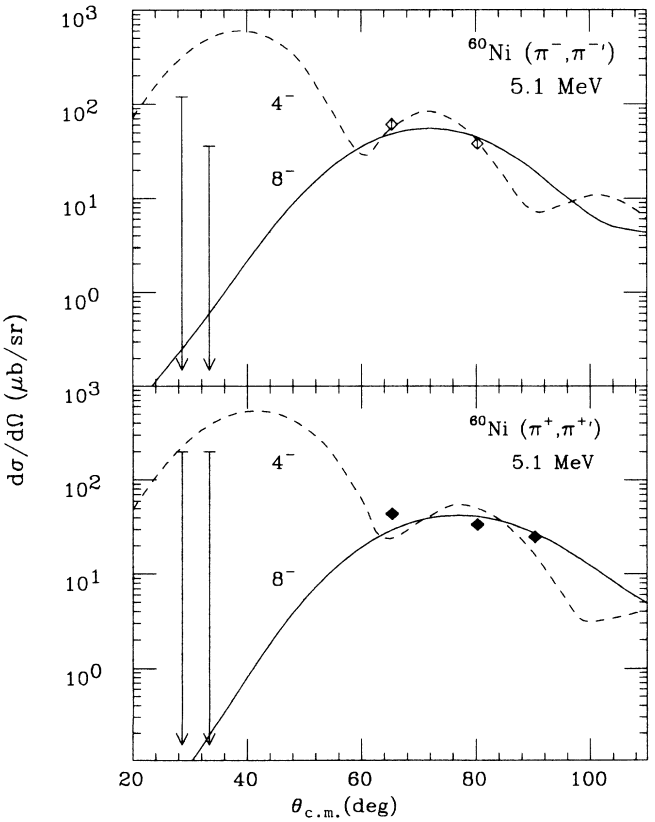

FIG. 3. The 5.1 MeV data are compared to DWIA calculations using the HO parameter $b = 1.95$ fm for 8^- and 4^- states. The curves have been adjusted to fit our large angle data. The 30° and 35° upper limits are from Oakley *et al.* (Ref. 28).

The ratio of the π^+ and π^- isoscalar to isovector strength near resonance of the dominant spin-orbit coupling term is well known from $\pi^{\pm}$-p scattering, and we have assumed that the uncertainties in this ratio are much less than the large fluctuations observed in the extracted values of the overall normalization N. This also implies that the overall normalization factor is the same in π^+ and π^- scattering. Any multistep process in the interaction is assumed to be included in the optical model parameters used to describe the distorted waves.

For purposes of illustrating the important features that relate pion scattering and electron scattering for stretched transitions ($0^+ T_i \rightarrow J^{\pi} T_f$) we write the cross section in plane-wave Born approximation as a sum over the product of a spectroscopic coefficient Z_τ, the transverse spin density $\rho^{s\perp}_{J\tau}$, and the pion- (electron-) nucleon $G^{\pi}_{\tau}(G^{e}_{\tau})$ coupling factor:

$$\frac{d\sigma}{d\Omega} = \left| \sum_{\tau=0,1} Z_\tau \rho^{s\perp}_{J\tau} G^{\pi,e}_{\tau} \right|^2 , \tag{1}$$

where

$$Z_\tau = \langle J_f, T_f || (a^{\dagger}_{ja} \times \bar{a}_{j_b})^{J\tau} || J_i = 0, T_i \rangle , \tag{2}$$

$$\rho^{s\perp}_{J\tau}(q) = \left[\frac{J+1}{2J+1} \right]^{1/2} \int_0^{\infty} \rho_\tau(r) j_{J-1}(qr) r^2 dr , \tag{3}$$

$$G^{\pi}_{\tau} = \sqrt{4\pi(2J+1)} \left[\frac{\mu}{2\pi\hbar^2} \right] \bar{t}^{\tau}_{s\perp} , \tag{4}$$

where $\bar{t}^{\tau}_{s\perp}(q)$ is the spin-orbit pion-nucleon interaction near resonance, $\rho_\tau(r)$ is the spin transition density, and J is the total angular momentum.

The transition density $\rho_\tau(r)$ was calculated from HO and WS wave functions. The WS wave functions, including those for unbound states, were generated by the computer code DWUCK4,[31] as defined in previous work on stretched transitions.[12] This transition density was used as input to the general inelastic scattering potential code ALLWRLD (Ref. 32) to generate pion form factors for input to the pion distorted-wave code MSUDWPI (Ref. 33). The optical potential in MSUDWPI is based on the one described by Stricker, McManus, and Carr.[34,35]

The ground state density parameters used in both codes and listed in Table II were based on the charge radius[36] and taken from previous fits of elastic pion scattering data.[27,37–39] We checked these parameters in our codes by fitting elastic pion scattering data from ^{16}O, ^{28}Si, and ^{60}Ni and found our c and a to be the same within about 5%. Using these different ground state density parameters would change the normalization for the stretched states by 1% or less. The spin-orbit force parameters used in ALLWRLD were $S_0=0.24+0.48i$ and $S_1=0.14+0.24i$ for 162 MeV pions.[40] Optical potential parameters[40,41] used in MSUDWPI are listed in Table III. When these values for the spin-orbit force and the optical potential were replaced by another set of values,[15] the resulting theoretical matrix element for the 11.7 MeV state in ^{14}C was about 5% smaller. These parameters gave DWIA calculations that fit the elastic scattering pion data reasonably well at forward angles in ^{28}Si.

In calculating the single-particle wave functions, the b for HO and the r_0, a, and λ for WS, were taken from fits to the electron scattering cross sections for stretched states.[12] The WS wave functions used the potential

$$U=-V_0 f+V_0\lambda(\hbar/2Mc)^2(\sigma\cdot l)r^{-1}df/dr\ ,$$

where

$$f=\{1+\exp[(r-r_0A^{1/3})/a]\}^{-1}\ .$$

In DWUCK4,[31] the potential well depth is allowed to vary and was not an input parameter.

For calculational purposes in Sec. III B, we write Eq. (1) for $\pi^{\pm}$ scattering in the DWIA for transitions where both isoscalar and isovector terms contribute as

$$\sigma^{\pm}=N^{\pm}f^2_{\text{c.m.}}(M_1^{\pm})^2\left[\frac{M_0^{\pm}}{M_1^{\pm}}Z_0+Z_1\right]^2\ , \tag{5}$$

where $M_\tau^{\pm}=\rho_{J_T}^{s\downarrow}G_\tau^{\pi^{\pm}}$. Note that $(M_\tau^{\pm})^2$ is the DWIA calculated cross section for pure isoscalar or isovector transitions. We have also included a factor $N^{\pm}f^2_{\text{c.m.}}$ composed of a center-of-mass term $f_{\text{c.m.}}$ and an empirical normalization $N^{\pm}$ defined such that the pion DWIA calculated cross section agrees with experimental strengths known by electron scattering. In this work it is assumed that the empirical normalization factor is the same for π^+ and π^- scattering, i.e., $N^+=N^-=N$.

The center-of-mass correction is included in the HO analysis of pion scattering by using a modified parameter $b'=b[(A-1)/A]^{1/2}$ in the wave function calculations, where b is the usual HO parameter. The final theoretical cross section is then adjusted by the c.m. factor,[15,42] $f^2_{\text{c.m.}}=[A/(A-1)]^L$. In the WS calculations it is not clear how to make the c.m. correction; therefore, the final theoretical cross section is adjusted by this same c.m. factor $f^2_{\text{c.m.}}$.

In electron scattering plane-wave Born approximation, the cross section is written as

$$\frac{d\sigma}{d\Omega}=\frac{Z^2\sigma_M}{1+(2E_0/M_T)\sin^2\theta/2}\left[\frac{q_\mu^2}{2q^2}+\tan^2\theta/2\right]F_T^2(q)\ , \tag{6}$$

where the form factor $F_T^2(q)$ is now written in exactly the same form as Eq. (1) with Z_τ and $\rho_{J_\tau}^{s\downarrow}$ defined as in Eqs. (2) and (3) and the electron-nucleon coupling factor G_τ^e is defined as

$$G_\tau^e=\sqrt{4\pi(2J+1)}/Z\left[\frac{q\hbar}{2mc}\right]\frac{1}{2}g_\tau^s\ , \tag{7}$$

where g_0^s (g_1^s) is the sum (difference) of the neutron and proton magnetic moments.

Again for calculational purposes, we write the electron scattering form factors in a form analogous to Eq. (5):

$$F_T^2=(M_1^e)^2\left[\frac{M_0^e}{M_1^e}Z_0+Z_1\right]^2\ , \tag{8}$$

where nucleon finite size and center-of-mass factors are contained in the isovector and isoscalar electromagnetic matrix elements M_1^e and M_0^e as defined in Ref. 12. Distorted-wave Born approximation effects are included in the standard q_{eff} approximation.

B. Determination of spectroscopic amplitudes Z_1 and Z_0 and normalization factors N

We use the experimental pion and electron scattering cross sections at the peak of the angular distribution as determined using a χ^2 fit of calculations to the data. For pion scattering, the $\sigma^{\pm}/(M_1^{\pi})^2$ ratio was varied for each state independently. The resulting $\sigma^{\pm}$ at the peak of the form factor and used in Eq. (5) are listed in Table IV.

TABLE II. Ground state density distribution parameters used in ALLWRLD and MSUDWPI. All quantities are in units of fm.

Nucleus	$\langle r^2\rangle_{\text{ch}}^{1/2}$[a]	$\langle r^2\rangle_{\text{nm}}^{1/2}$[a]	c[b]	a[b]
^{14}C	2.56	2.43	2.52	0.39
^{28}Si	3.12	3.02	2.86	0.55
^{54}Fe	3.70	3.61	3.84	0.55
^{60}Ni	3.80	3.71	4.00	0.55

[a]The charge radius is from electron scattering (Ref. 36) and the nuclear matter radius is from $\langle r^2\rangle_{\text{nm}}=\langle r^2\rangle_{\text{ch}}-(0.8)^2$.

[b]The ground state distributions were assumed to have a Woods-Saxon form $\rho(r)\propto(1+e^{(r-c)/a})^{-1}$. The radius c and diffuseness a are taken from previous pion scattering analyses (Refs. 27, 37, 38, and 39) and use the relation $\frac{5}{3}\langle r^2\rangle_{\text{nm}}=c^2+\frac{7}{3}\pi^2a^2$.

TABLE III. The optical potential parameters used in MSUDWPI (see Refs. 15, 35, 40, and 41) for 162 MeV incident pions.

	Incoming	Outgoing
$\bar{b}_0$ (fm)	$-0.083+0.029i$	$-0.079+0.027i$
b_1 (fm)	$-0.125+0.003i$	$-0.126+0.002i$
c_0 (fm^3)	$+0.37\ +0.67i$	$+0.56\ +0.62i$
c_1 (fm^3)	$+0.21\ +0.33i$	$+0.31\ +0.31i$
B_0 (fm^4)	$-0.15\ +0.28i$	$-0.13\ +0.26i$
C_0 (fm^6)	$+1.29\ +2.95i$	$+1.15\ +2.55i$

TABLE IV. Experimental cross sections (in μb/sr) at the top of the angular distribution arrived at by doing a least-squares fit to the data. For comparison, form factors from electron scattering are also given (Ref. 12).

	Ref.	J^π	T	E_x (MeV)	σ^- (μb/sr)	σ^+ (μb/sr)	F^2 ($\times 10^{-5}$)
^{14}C	43	4^-	1	11.7	67± 4	<6	21.6±1.4
			1	15.2	14± 3	30±2	
			1	17.3	<16	123±4	26.0±2.6
^{28}Si	8	6^-	0	11.6	31± 4	35±2	
			1	14.4	17± 4	23±2	10.0±0.2
^{54}Fe	17	8^-	1	8.3	13.7± 1.6	0.9±0.6	0.29±0.02
			1	8.9	3.7± 0.3	2.7±0.5	0.26±0.02
			1	9.8	7.7± 1.3	5.6±1.5	
			1	10.0	4.3± 1.1	8.1±0.6	0.31±0.01
			1	10.7	7.8± 2.3	17.7±1.0	0.29±0.03
			1	11.6	5.5± 1.1	2.1±0.5	
			2	13.3	15.6± 1.9	13.2±1.1	1.34±0.07
^{60}Ni		8^-	2	5.1	55.0±11.0	42.0±8.0	
			2	7.5	8.7± 1.2	10.0±1.0	0.34±0.02
			2	9.0	4.2± 0.4	7.7±0.8	0.18±0.01
			2	9.2	6.9± 1.9	7.0±2.1	0.17±0.01
			3	13.9	9.3± 4.9	4.6±0.1	0.31±0.02

For electron scattering, the F_T^2 was determined in Ref. 12 by a similar procedure. The resulting F_T^2, including meson exchange current (MEC) effects, used in Eq. (8) are listed in Table IV.

The $(M_1^\pm)^2 (=\sigma_{\rm IDW}^\pm$, for $Z_0=0$ and $Z_1=1$) cross sections were calculated by ALLWRLD and MSUDWPI using both HO and WS wave functions and some representative results are given in Table V. The matrix elements are much smaller for π^+ than for π^- in cases where the unbound proton has been treated correctly by using different WS wave functions for the unbound proton than for the bound neutron. In the past, the use of equal proton and neutron HO wave functions has predicted approximately equal π^+ and π^- matrix elements. This difference is important in determining whether a stretched transition is to a pure isovector T_0+1 state based on a comparison of the π^+ and π^- cross sections. The $(M_1^e)^2$ were calculated as in Ref. 12, but included MEC effects.

The M_0^e/M_1^e ratio in Eq. (8) for electron scattering is small (-0.187 when using HO wave functions) and thus magnetic electron scattering mainly probes the isovector transitions. When using WS wave functions, the neutron and proton wave functions are not equal and the M_0^e/M_1^e ratio is explicitly calculated.[12] On the other hand, $M_0^{\pi^\pm}/M_1^{\pi^\pm} \approx \mp 2$ in Eq. (5) for pion scattering near the $\Delta_{3,3}$ resonance and thus pion scattering is more sensitive to isoscalar transitions. From ALLWRLD and MSUDWPI calculations this ratio was found to be 1.93 for 162 MeV incident pions, when using HO wave functions. When using WS wave functions the ratio varied from 1.7 to 2.2 for different transitions, but for a given transition, the ra-

TABLE V. These representative DWIA pion cross sections, $(M_1^\pi)^2$, at the peak of the angular distribution were used in Eq. (5) and were calculated by ALLWRLD and MSUDWPI.

			Binding energy		HO		WS	
	J^π	E_x (MeV)	n (MeV)	p (MeV)	$(M_1^{\pi^-})^2$ (μb/sr)	$(M_1^{\pi^+})^2$ (μb/sr)	$(M_1^{\pi^-})^2$ (μb/sr)	$(M_1^{\pi^+})^2$ (μb/sr)
^{14}C	4^-	11.7	−0.16	−9.13	62.7	69.1	72.9	38.9
		15.2	+3.34	−5.63	60.7	66.7	82.3	47.9
		17.3	+5.44	−3.53	59.0	65.0	99.8	34.0
^{28}Si	6^-	11.6	−5.59	0.00	73.4	64.8	64.2	65.8
		14.4	−2.81	+2.78	70.9	62.4	70.7	45.8
^{54}Fe	8^-	8.3	−5.07	−0.54	49.4	42.2	48.6	42.5
		10.7	−2.70	+1.83	47.7	40.8	54.5	28.6
		13.3	−4.38	+4.41	46.4	39.4	49.6	31.6
^{60}Ni	8^-	7.5	−7.77	−2.01	41.9	37.0	38.6	38.9
		9.2	−6.12	−0.36	41.0	36.1	38.9	39.1
		13.9	−4.83	+4.38	38.7	34.0	40.3	29.7

tio varied by less than 10% over the range of scattering angles. In ^{14}C however, M_0^π and M_1^π peaked at scattering angles that were about 15° different, making it impossible to use some average M_0^π/M_1^π ratio. In this case the angular distribution of the data was fit using $M_n=(M_0+M_1)/\sqrt{2}$ for the 11.7 MeV state, $M_p=(M_0-M_1)/\sqrt{2}$ for the 17.3 MeV state, and M_0 for the 15.2 MeV state.

Using these known values, Eqs. (5) and (8) are solved for Z_0, Z_1, and N, where we assume that $N=N^+=N^-$. Two different computational methods were used depending on what cross sections were known.

(i) If all three experimental cross sections are known for a given state, we have three equations and three unknowns: Z_0, Z_1, and N. The Z coefficients can be determined independent of our ability to calculate absolute pion scattering cross sections as long as the relative π^+ and π^- strengths are known. The following *ratio method* is dependent only on the well known relative π^+/π^- cross section and M_0/M_1 ratio near $\Delta_{3,3}$ resonance energies. The Z_0/Z_1 ratio is found in terms of $R=\sigma^+/\sigma^-$ from Eq. (5). The two possible solutions are

$$\frac{Z_0}{Z_1}=-\frac{M_1^+\pm M_1^-\sqrt{R}}{M_0^+\pm M_0^-\sqrt{R}}\ . \tag{9}$$

For $M^+\approx M^-$, we see that the Z_0/Z_1 ratio is dependent only on the M_0/M_1 ratio and not on the actual value of the matrix element. The Z_0 and Z_1 coefficients are determined by simultaneously solving Eqs. (8) and (9) (where we arbitrarily use the positive square root for Z_1). Since there are two solutions for Z_0/Z_1, there will be two sets of Z coefficients independent of the pion normalization. After the Z coefficients are known, Eq. (5) can be solved for the normalization factor N; one for each Z_0/Z_1 solution.

(ii) In some cases only two of the three cross sections are well known, and it is necessary to assume some normalization in the *absolute method.* We then have two equations and two unknowns:

$$Z_i=\frac{R_x M_j^y\pm R_y M_j^x}{M_i^y M_j^x-M_i^x M_j^y}\ , \tag{10}$$

where i and j (with $i\neq j$) are 0,1 for isoscalar and isovector components and x and y are any two of the three scattering reactions such that $R_e=\sqrt{F^2}$ and $R_{\pi^\pm}=\sqrt{\sigma^\pm/N^\pm f_{\text{c.m.}}^2}$.

In all the calculations, the Z_1 coefficient is mainly determined by electron scattering, so that the Z_1 calculated here, with pion scattering cross sections included, is not appreciably different from that calculated previously ($|F/M_1^e|$) using only electron scattering cross sections.[12] The magnitude of Z_1 is inversely proportional to the size of the electron scattering matrix element. The magnitude of Z_0, on the other hand, is determined relative to Z_1, from the well known ratio between π^+ and π^- cross sections as defined in $R=\sigma^+/\sigma^-$. Thus, the magnitude of Z_0 is not proportional to the pion scattering matrix element; only the normalization N is proportional to this matrix element.

IV. DISCUSSION OF RESULTS

Pion angular distributions calculated from MSUDWPI using best fit parameters are compared to pion data for stretched 8^- transitions in ^{60}Ni in Fig. 2 and for selected stretched transitions in ^{14}C, ^{28}Si, and ^{54}Fe in Fig. 4. Using peak cross sections from the fitted angular distributions, the Z coefficients tabulated in Table VI were extracted using transition densities calculated from HO and WS wave functions. The quality of the data is insufficient to resolve differences in the angular distributions, and therefore we conclude that the data are fit equally well with HO or WS wave functions. We also notice that the extracted Z_0 and Z_1 coefficients are independent (within experimental error) of whether HO or WS wave functions were employed.

We used the pure $T=1$ transition to the $J^\pi=6^-$, $E_x=14.4$ MeV state in ^{28}Si as a check of our pion scattering calculations. Using the oscillator parameter and Z_1 coefficient determined from fitting the electron transition to this state resulted in a normalization factor of 1.0±0.1, which is consistent with other work[5] where a factor of 1.15 was found.

As discussed previously for $T=1\rightarrow T=1$ transitions, two solutions for Z_0 and Z_1 are always possible. In ^{14}C the ratio method yields two values of Z_0 and Z_1 for each of the 11.7 and 17.3 MeV states. One set has normalizations of 1.1 and 2.6, respectively. (The other set, yielding more unfavorable factors of 4.5 and 9.3, was rejected.)

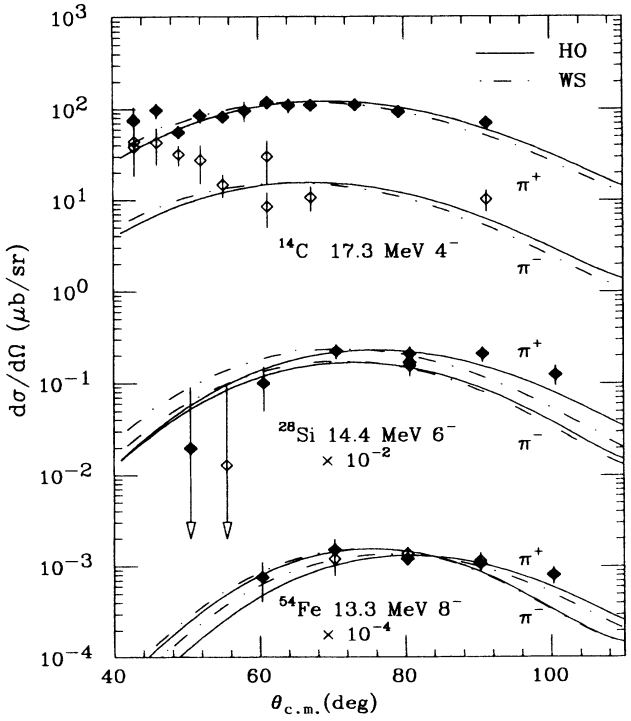

FIG. 4. Pion angular distributions calculated with HO and WS wave functions are compared to the data for stretched transitions in ^{14}C, ^{28}Si, and ^{54}Fe. Open diamonds are the π^- data; solid diamonds are the π^+ data.

Because the π^+ data is poor for the 11.7 MeV state, and the π^- data is poor for the 17.3 MeV state, the absolute method was then used with an average normalization of $N=1.7$ to determine the Z coefficients. The normalization factor of 1.7 is different from the $N=1.4$ determined previously[4,40,43] for ^{14}C because a different harmonic oscillator parameter and ground state density were used in the theoretical calculations. In addition, shell model calculations by Millener and Kurath[15] predict two strong $T=1$ $J^\pi=4^-$ states at 12.1 and 16.4 MeV. The lower excited state is calculated to be primarily a neutron particle-hole excitation while the upper state is primarily a proton excitation. This is also consistent with the experimentally extracted values of Z_0 and Z_1 shown in Table IV and inconsistent with the rejected set based on the large normalization factors.

In ^{54}Fe, mixed isoscalar and isovector $M8$ transitions from the $T=1$ ground state to the excited states at 8.3, 8.9, 10.0, and 10.7 MeV also have two solutions. Since we know the $M8$ transition to the $E_x=13.3$ MeV state is purely isovector ($T=2$), we assume that a normalization of 2.1 is typical for ^{54}Fe. Shell model calculations performed for 8^- states in a $(g_{9/2}f_{7/2}^{-3})$ basis[17] predict the lowest excited state to be predominantly a neutron excitation which is consistent with the solution for the 8.3 MeV state in Table VI, but in disagreement with Geesaman *et al.*[17] We believe that our second solution which corresponds to an almost pure isovector transition is unreasonable, because it leads to a larger normalization factor of 2.9 and is in disagreement with results from shell model calculations which generally predict the lowest state to be almost pure neutron. For the 8.9, 10.0, and 10.7 MeV states we reject the solutions with normalization of 0.1, 0.3, and 8.8, respectively.

In ^{60}Ni the interesting feature is that most of the transitions are dominantly isovector with the exception of the 5.1 MeV state, which is dominantly isoscalar. However, nuclear structure calculations are not available for comparison. A serious concern here is that the extracted normalization factor is about twice as large as in ^{14}C and ^{54}Fe. Even though the background is large compared to the peaks shown in Fig. 1, the uncertainties on the peak cross sections are still much less than that needed to bring the large normalization factor into agreement with the light nuclei.

An interesting observation for purely isovector or purely isoscalar stretched states is that the calculated $\sigma(\pi^-)/\sigma(\pi^+)$ ratio is approximately equal to unity only when using HO wave functions (see Table V). Experimentally, this ratio is significantly different than unity in a number of cases as shown in Figs. 2 and 4 and listed in Table IV. In particular, the experimental π^- and π^+ cross sections for the 13.9 MeV state in ^{60}Ni are definitely not equal. (This observation is only important of course if the 13.9 MeV stretched state is in fact a T_0+1 state, which we have assumed.) This feature can be attributed to having the proton much more unbound for this high-spin state than the neutron. When the unbound nature of the nucleons is included in the WS wave functions, the relative cross sections are better reproduced. This asymmetry seen in the ^{60}Ni data has been previously demonstrated for giant quadrupole resonances.[44]

TABLE VI. A tabulation of Z coefficients for stretched states extracted from simultaneous analysis of both electron and pion scattering. The Z_1 coefficients have arbitrarily been chosen to be the positive solution. The states denoted by an asterisk were only observed in pion scattering. In these cases, the Z coefficients were determined by the absolute method using an average N from the other states in that nucleus, except in ^{54}Fe where the N from only the strong 13.3 MeV state was used.

			HO			WS		
	E_x (MeV)	T	Z_0	Z_1	N	Z_0	Z_1	N
^{14}C[a]	11.7	1	0.21±0.03	0.30±0.01	1.7±0.3	0.19±0.03	0.29±0.02	2.0±0.3
	15.2*	1	−0.20±0.01	0.07±0.03	1.7±0.3	−0.21±0.02	0.08±0.03	2.0±0.3
	17.3	1	−0.38±0.04	0.22±0.02	1.7±0.3	−0.39±0.04	0.22±0.02	2.0±0.3
^{28}Si[b]	11.6*	0	−0.32±0.02	0.03±0.04	1.0±0.2	−0.34±0.03	0.03±0.05	1.0±0.2
	14.4	1	−0.03±0.02	0.49±0.01	1.0±0.2	−0.05±0.03	0.55±0.01	1.0±0.2
^{54}Fe[c]	8.3	1	0.19±0.03	0.21±0.01	0.8±0.2	0.18±0.03	0.21±0.01	0.8±0.2
	8.9	1	0.00±0.01	0.16±0.01	2.3±0.3	−0.01±0.01	0.17±0.01	2.4±0.4
	9.8*	1	0.13±0.01	0.01±0.02	2.1±0.3	0.14±0.01	0.00±0.03	2.0±0.3
	10.0	1	−0.02±0.01	0.18±0.01	3.9±0.6	−0.03±0.01	0.19±0.01	3.9±0.7
	10.7	1	−0.27±0.11	0.12±0.02	0.9±0.6	−0.27±0.11	0.14±0.02	1.1±0.7
	11.6*	1	0.10±0.01	0.04±0.02	2.1±0.3	0.10±0.01	0.04±0.02	2.0±0.3
	13.3	2	0.00±0.01	0.37±0.01	2.1±0.3	−0.02±0.01	0.41±0.01	2.0±0.3
^{60}Ni	5.1*	2	0.23±0.02	0.02±0.03	5.5±0.6	0.23±0.02	0.02±0.03	5.7±0.6
	7.5	2	−0.01±0.01	0.20±0.01	5.2±0.6	0.00±0.01	0.20±0.01	5.5±0.6
	9.0	2	−0.01±0.01	0.15±0.01	6.5±0.9	−0.01±0.01	0.14±0.01	6.5±0.9
	9.2	2	0.00±0.01	0.14±0.01	7.9±2.8	0.00±0.01	0.14±0.01	8.0±2.6
	13.9	3	0.01±0.01	0.20±0.01	4.2±1.1	0.01±0.01	0.21±0.01	3.8±1.1

[a]See Refs. 15 and 43.
[b]See Ref. 5.
[c]See Ref. 17.

The wide variation in normalization factors observed in Table VI is not understood, suggesting that we do not completely understand pion scattering from nuclei. In general, there could be ambiguities associated with the transition density, the optical model potential, the strength of the spin-orbit interaction in the nuclear medium, or even the DWIA itself. Since the transition density is taken from electron scattering measurements and $\Delta N \geq 3\hbar\omega$ contributions are negligible as discussed earlier, uncertainties associated with the spin density are much smaller than that required to account for the large normalization factors, particularly for ^{54}Fe and ^{60}Ni. Moreover, from a comparison of results using HO and WS wave functions shown in Table VI changes in the radial wave function due to the fact that the proton and neutron wave function are different, particularly for states unbound to protons or neutrons, cannot account for the large variation in the normalizations. Reasonable changes in the optical potential parameters in Table III did not affect large changes in the total cross section. Although the total pion cross section is sensitive to the oscillator parameter b, values were taken from fitting the electron scattering data in all cases. The parameters defining the ground state matter distribution were taken from fitting the pion elastic scattering and the ground state charge radius from elastic electron scattering. Although the total cross section is sensitive to these parameters, we have deduced them in the standard way and employed them in a systematic manner.

The remaining uncertainty is the strength of the spin-orbit interaction in the nucleus, but it still would be surprising to see such large variations in the strength due to the nuclear medium in passing from ^{54}Fe to ^{60}Ni. Although, the quality of the pion data is not good, it is sufficient on the average to conclude that there is an unexplained enhancement of the observed pion cross section for these transitions.

In a shell model space where the stretched transitions are excited by a one-body operator and invoking closure, the square of the isoscalar and isovector amplitudes separately obey certain sum rules.[12] For the T_0 states the sum rule is

$$\sum_i (Z_1^i)^2 = \frac{1}{2J}\left[n_n + \left[\frac{T_0-1}{T_0+1}\right] n_p\right] . \tag{11}$$

For T_0+1 states the sum rule is

$$\sum_i (Z_1^i)^2 = \frac{1}{2J}\left[\frac{2}{T_0+1} n_p\right] . \tag{12}$$

The total sum rule for the isovector Z coefficients is then

$$\sum_i (Z_1^i)^2 = \frac{1}{2J}(n_n+n_p) = \frac{n}{2J} . \tag{13}$$

Further constraints on the Z coefficients are $\sum_i (Z_0^i Z_1^i) = (n_n - n_p)/2J$, $\sum_i (Z_n^i)^2 = n_n/J$, and $\sum_i (Z_p^i)^2 = n_p/J$. We define n_n and n_p as the number of neutrons and protons respectively in the orbital j_h from which the nucleon is promoted and $n = n_n + n_p$, T_0 as the isospin of the nuclear ground state, and $J = 2j_h + 1$ for stretched transitions. Note that in general $n = 2J$ for a full orbital. Equation (13) is also the sum rule for the isoscalar Z coefficients, $\sum_i (Z_0^i)^2$, to T_0 states only.

The sums of the squares of the Z coefficients derived using WS wave functions and the limits given by the sum rule from Eqs. (11), (12), and (13) are tabulated in Table VII. We have also tabulated in Table VII the ratio $S_\tau^2 = \sum(Z_\tau^2)_{\rm exp} / \sum(Z_\tau^2)_{\rm thy}$. As shown graphically in Fig. 5, the total isoscalar and isovector strength is significantly less than that predicted by the sum rule ($S^2 \ll 1$), with the isoscalar strength quenched even more than the isovector strength. Including MEC effects for electron scattering increases the calculated matrix elements by 15% to 20%, which increases the quenching in all cases.[12]

The isoscalar strength in ^{60}Ni was found to be only 22% of the isovector strength. If the questionable new 8^- isoscalar state of 5.1 MeV (not observed in electron scattering) is not included, the isoscalar strength would be less than 1% of the isovector strength.

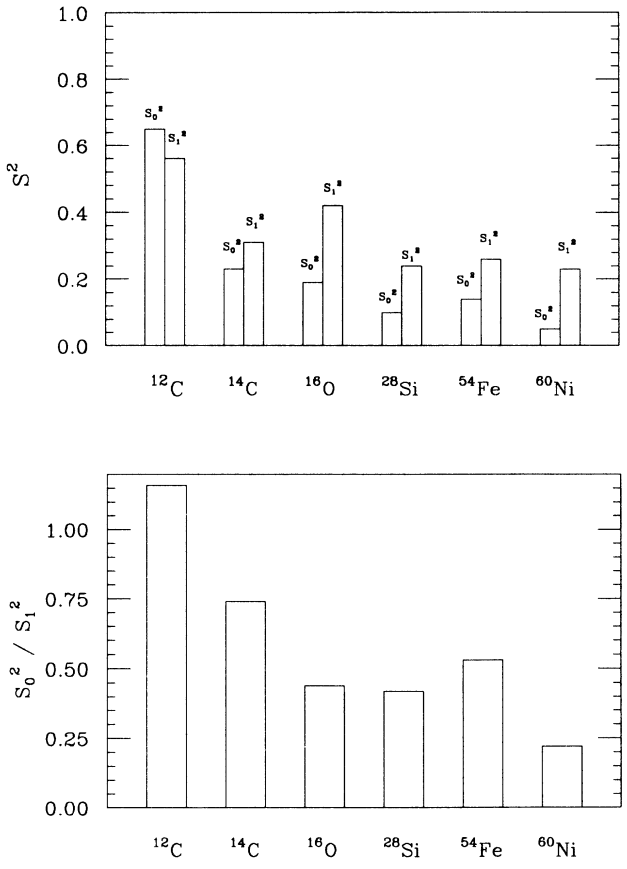

FIG. 5. A bar graph showing the quenching of isoscalar (S_0^2) and isovector (S_1^2) strengths for the six nuclei where both electron and pion scattering to the stretched states have been carried out. No quenching corresponds to 1.0. The HO values plotted are total S_0^2 and total S_1^2 from Table VII. Also plotted is a display of the ratio of isoscalar to isovector quenching, where S_0^2/S_1^2 is from Table VII. Equal quenching corresponds to 1.0.

TABLE VII. Sums of Z coefficients squared. The experimental values are sums for HO wave functions from Table VI. The theoretical values are calculated from the sum rules of Eqs. (11)–(13). The ratio of experiment to theory is defined as $S_\tau^2=\sum(Z_\tau^2)_{\rm exp}/\sum(Z_\tau^2)_{\rm thy}$. For completeness, we have included the two other even-even nuclei, ^{12}C and ^{16}O, where the stretched states have been studied by both pion and electron scattering (Refs. 6, 7, 45, and 46).

		Experimental		Theoretical				
	T	$\sum Z_0^2$	$\sum Z_1^2$	$\sum Z_0^2$	$\sum Z_1^2$	S_0^2	S_1^2	S_0^2/S_1^2
^{12}C	0				0			
	1				1			
	Total	0.65	0.56	1	1	0.65	0.56	1.16
^{14}C	1		0.14		$\frac{1}{2}$		0.29	
	2		0.17		$\frac{1}{2}$		0.34	
	Total	0.23	0.31	1	1	0.23	0.31	0.74
^{16}O	0				0			
	1		0.42		1		0.42	
	Total	0.19	0.42	1	1	0.19	0.42	0.44
^{28}Si	0				0			
	1		0.24		1		0.24	
	Total	0.10	0.24	1	1	0.10	0.24	0.42
^{54}Fe	1		0.12		$\frac{1}{2}$		0.24	
	2		0.14		$\frac{3}{8}$		0.37	
	Total	0.14	0.26	$\frac{7}{8}$	$\frac{7}{8}$	0.16	0.29	0.53
^{60}Ni	2		0.10		$\frac{2}{3}$		0.15	
	3		0.13		$\frac{1}{3}$		0.39	
	Total	0.05	0.23	1	1	0.05	0.23	0.22

V. CONCLUSIONS

The normalization factor for acceptable solutions to the pion scattering and electron scattering data varied from 1 to 5 for the four nuclei studied. The observation that this normalization factor departs from unity by such large factors suggest that there are serious discrepancies with the model. Although we understand the pion-nucleon interaction in free space quite well, it appears that the DWIA model of the pion-nucleon interaction inside the nucleus is more uncertain. However, the extraction of Z_0 and Z_1 from the ratio of π^+ to π^- cross sections is independent of this ambiguity, since it is only the relative cross section that matters. It was determined that the ratio of the total isoscalar to the total isovector strength ranged from $S_0^2/S_1^2=0.2$ to 1.2.

The use of WS wave functions in the pion scattering analysis did not substantially change the Z_0/Z_1 ratio from that found using HO wave functions. However, the actual magnitude of Z_0 is larger, since it is based on the larger Z_1 calculated using WS wave functions on electron scattering data.[12] For all nuclei, the use of WS wave functions predicts unequal π^+ and π^- cross sections for unbound isovector states and better reproduced the asymmetry in the isovector 13.9 MeV state of ^{60}Ni. The prediction of asymmetric cross sections suggests a need for care in making isospin assignments based on equal π^+ and π^- cross sections.

ACKNOWLEDGMENTS

We thank E. S. Rost for helpful suggestions, S. Greene for overseeing the fabrication of the ^{60}Ni target, A. Petit for help with the data analysis, and D. Oakley for analyzing and sharing 180 MeV pion scattering ^{60}Ni spectra at small angles. This work was supported in part by the U.S. Department of Energy.

*Present address: Institute of Nuclear and Particle Physics and Physics Department, University of Virginia, Charlottesville, VA 22901.

†Present address: Department of Physics, Harvard University, Cambridge, MA 02138.

[1] R. A. Lindgren and F. Petrovich, in *Spin Excitations in Nuclei*, edited by F. Petrovich *et al.* (Plenum, New York, 1984), p. 323.

[2] F. Petrovich and W. G. Love, Nucl. Phys. **A354**, 499c (1981).

[3] F. Petrovich, J. A. Carr, and H. McManus, Annu. Rev. Nucl. Part. Sci. **36**, 29 (1986).

[4] M. A. Plum, R. A. Lindgren, J. Dubach, R. S. Hicks, R. L. Huffman, B. Parker, G. A. Peterson, J. Alster, J. Lichtenstadt, M. A. Moinester, and H. Baer, Phys. Rev. C **40**, 1861 (1989).

[5] J. A. Carr, F. Petrovich, D. Halderson, D. B. Holtkamp, and

W. B. Cottingame, Phys. Rev. C **27**, 1636 (1983).
[6]R. S. Hicks, J. B. Flanz, R. A. Lindgren, G. A. Peterson, L. W. Fagg, and D. J. Millener, Phys. Rev. C **30**, 1 (1984).
[7]C. E. Hyde-Wright, W. Bertozzi, T. N. Buti, J. M. Finn, F. W. Hersman, M. V. Hynes, M. A. Kovash, J. J. Kelly, S. Kowalski, J. Lichtenstadt, R. W. Lourie, B. E. Norum, B. Pugh, C. P. Sargent, B. L. Berman, F. Petrovich, and J. A. Carr, Phys. Rev. C **35**, 880 (1987).
[8]C. Olmer, B. Zeidman, D. F. Geesaman, T.-S. H. Lee, R. E. Segel, L. W. Swenson, R. L. Boudrie, G. S. Blanpied, H. A. Thiessen, C. L. Morris, and R. E. Anderson, Phys. Rev. Lett. **43**, 612 (1979).
[9]S. Krewald and J. Speth, Phys. Rev. Lett. **45**, 417 (1980).
[10]J. Lichtenstadt, J. Heisenberg, C. N. Papanicolas, C. P. Sargent, A. N. Courtemanche, and J. S. McCarthy, Phys. Rev. C **20**, 497 (1979).
[11]D. Halderson, R. J. Philpott, J. A. Carr, and F. Petrovich, Phys. Rev. C **24**, 1095 (1981).
[12]B. L. Clausen, R. J. Peterson, and R. A. Lindgren, Phys. Rev. C **38**, 589 (1988).
[13]S. Yen, R. Sobie, H. Zarek, B. O. Pich, T. E. Drake, C. F. Williamson, S. Kowalski, and C. P. Sargent, Phys. Lett. **93B**, 250 (1980).
[14]M. A. Plum, R. A. Lindgren, J. Dubach, R. S. Hicks, R. L. Huffman, B. Parker, G. A. Peterson, J. Alster, J. Lichtenstadt, M. A. Moinester, and H. Baer, Phys. Lett. **137B**, 15 (1984).
[15]M. A. Plum, Ph.D. thesis, University of Massachusetts, Amherst, 1985.
[16]D. B. Holtkamp, S. J. Seestrom-Morris, S. Chakravarti, D. Dehnhard, H. W. Baer, C. L. Morris, S. J. Greene, and C. J. Harvey, Phys. Rev. Lett. **47**, 216 (1981).
[17]D. F. Geesaman, R. D. Lawson, B. Zeidman, G. C. Morrison, A. D. Bacher, C. Olmer, G. R. Burleson, W. B. Cottingame, S. J. Greene, R. L. Boudrie, C. L. Morris, R. A. Lindgren, W. H. Kelly, R. E. Segel, and L. W. Swenson, Phys. Rev. C **30**, 952 (1984).
[18]R. A. Lindgren, J. B. Flanz, R. S. Hicks, B. Parker, G. A. Peterson, R. D. Lawson, W. Teeters, C. F. Williamson, S. Kowalski, and X. K. Maruyama, Phys. Rev. Lett. **46**, 706 (1981).
[19]B. L. Clausen, Ph.D. thesis, University of Colorado, Boulder, 1987.
[20]R. A. Lindgren, M. A. Plum, W. J. Gerace, R. S. Hicks, B. Parker, C. F. Williamson, X. K. Maruyama, and F. Petrovich, Phys. Rev. Lett. **47**, 1266 (1981).
[21]H. A. Thiessen and S. Sobottka, Los Alamos Scientific Laboratory Report No. LA-4534-MS, 1970.
[22]R. J. Peterson, B. L. Clausen, J. J. Kraushaar, R. A. Lindgren, M. A. Plum, W. W. Jacobs, and H. Nann, Phys. Rev. C **35**, 495 (1987).
[23]R. A. Arndt and L. O. Roper, program SAID (Scattering Analysis Interactive Dialin), SM86.
[24]J. Piffaretti, R. Corfu, J.-P. Egger, P. Gretillat, C. Lunke, E. Schwarz, C. Perrin, and B. M. Preedom, Phys. Lett. **71B**, 324 (1977).
[25]S. J. Seestrom-Morris, Ph.D. thesis, University of Minnesota, Minneapolis, 1981.
[26]B. Chabloz, R. Corfu, J.-P. Egger, J.-F. Germond, P. Gretillat, C. Lunke, J. Piffaretti, E. Schwarz, C. Perrin, J. E. Bolger, and J. Zichy, Phys. Lett. **81B**, 143 (1979).
[27]C. Olmer, D. F. Geesaman, B. Zeidman, S. Chakravarti, T.-S. H. Lee, R. L. Boudrie, R. H. Siemssen, J. F. Amann, C. L. Morris, H. A. Thiessen, G. R. Burleson, M. J. Devereux, R. E. Segel, and L. W. Swenson, Phys. Rev. C **21**, 254 (1980).
[28]D. Oakley (private communication).
[29]H. Ronsin, P. Beuzit, J. Delaunay, R. Ballini, I. Fodor, and J. P. Fouan, Nucl. Phys. **A207**, 577 (1973).
[30]P. Blunden, B. Castel, and H. Toki, Z. Phys. A **312**, 247 (1983).
[31]P. D. Kunz, distorted-wave Born approximation code DWUCK4, University of Colorado.
[32]J. A. Carr, F. Petrovich, D. Halderson, and J. Kelly, scattering potential code ALLWRLD.
[33]J. A. Carr, distorted-wave code MSUDWPI; adapted from the code DWPI of R. A. Eisenstein and G. A. Miller, Comput. Phys. Commun. **11**, 95 (1976).
[34]K. Stricker, H. McManus, and J. A. Carr, Phys. Rev. C **19**, 929 (1979).
[35]K. Stricker, J. A. Carr, and H. McManus, Phys. Rev. C **22**, 2043 (1980).
[36]H. de Vries, C. W. de Jager, and C. de Vries, At. Data Nucl. Data Tables **36**, 495 (1987).
[37]M. Blecher, K. Gotow, R. Ng, R. L. Burman, R. Carlini, S. Dam, M. V. Hynes, M. J. Leitch, V. Sandberg, R. Auble, F. E. Bertrand, E. E. Gross, F. E. Obenshain, J. Wu, G. S. Blanpied, B. M. Preedom, B. G. Ritchie, W. Bertozzi, M. A. Kovash, and R. P. Redwine, Phys. Rev. C **25**, 2554 (1982).
[38]B. M. Preedom, S. H. Dam, C. W. Darden III, R. D. Edge, D. J. Malbrough, T. Marks, R. L. Burman, M. Hamm, M. A. Moinester, R. P. Redwine, M. A. Yates, F. E. Bertrand, T. P. Cleary, E. E. Gross, N. W. Hill, C. A. Ludemann, M. Blecher, K. Gotow, D. Jenkins, and F. Milder, Phys. Rev. C **23**, 1134 (1981).
[39]D. S. Oakley, M. J. Smithson, S. Mordechai, C. Fred Moore, P. A. Seidl, C. L. Morris, G. C. Idzorek, Z. F. Wang, R. Gilman, J. D. Zumbro, H. T. Fortune, S. J. Seestrom-Morris, K. S. Dhuga, and D. L. Watson, Phys. Rev. C **35**, 1392 (1987).
[40]J. A. Carr (private communication).
[41]J. A. Carr, in Workshop on Nuclear Structure with Intermediate-Energy Probes, edited by H. Baer *et al.*, Los Alamos Scientific Laboratory Report No. LA-8303-C, 1980.
[42]J. R. Comfort, G. L. Moake, C. C. Foster, P. Schwandt, C. D. Goodman, J. Rapaport, and W. G. Love, Phys. Rev. C **24**, 1834 (1981).
[43]D. B. Holtkamp, S. J. Seestrom-Morris , D. Dehnhard, H. W. Baer, C. L. Morris, S. J. Greene, C. J. Harvey, D. Kurath, and J. A. Carr, Phys. Rev. C **31**, 957 (1985).
[44]R. J. Peterson and J. L. Ullmann, Nucl. Phys. **A435**, 717 (1985).
[45]W. B. Cottingame, K. G. Boyer, W. J. Braithwaite, S. J. Greene, C. J. Harvey, R. J. Joseph, D. B. Holtkamp, C. Fred Moore, J. J. Kraushaar, R. J. Peterson, R. A. Ristinen, J. R. Shepard, G. R. Smith, R. L. Boudrie, N. S. P. King, C. L. Morris, J. Piffaretti, and H. A. Thiessen, Phys. Rev. C **36**, 230 (1987).
[46]D. B. Holtkamp, W. J. Braithwaite, W. Cottingame, S. J. Greene, R. J. Joseph, C. F. Moore, C. L. Morris, J. Piffaretti, E. R. Siciliano, H. A. Thiessen, and D. Dehnhard, Phys. Rev. Lett. **45**, 420 (1980).